Journal of Structural Geology, Vol. 3, No. 2, pp. 129 to 141, 1981
Printed in Great Britain

0191-8141/81/020129-12 $02.00/0
Pergamon Press Ltd

Comparison of quartz microfabric with strain in recrystallized quartzite

DAVID M. MILLER* and JOHN M. CHRISTIE

Department of Earth and Space Sciences, University of California, Los Angeles, CA 90024, U.S.A.

(*Received* 12 *May* 1980; *accepted in revised form* 19 *January* 1981)

Abstract—The relationship between quartz *c*-axis microfabric and strain is examined in six specimens of recrystallized quartzite conglomerate in which strain was measured using pebble shapes. Four rocks subjected to plane strain display a direct relationship between the strength of preferred orientation and the strain intensity. The *c*-axis distributions in these rocks, as well as a rock subjected to moderate extensional strain, are crossed-girdles with maxima near the intermediate principal strain axis and connecting girdles at acute angles to the direction of maximum shortening. A rock subjected to moderate flattening strain has several maxima clustered near the direction of maximum shortening and a weak connecting girdle through the intermediate principal strain axis.

These results are generally similar to those of other studies comparing strain and tectonite fabrics and also with experimental and computer simulation studies of fabrics. The degree of preferred orientation is related to total strain, and therefore microfabrics in quartzites may be cautiously interpreted as qualitative indicators of strain intensity. Uncertainties are greater, however, for correlations of fabric patterns with shapes of the strain ellipsoid. An observed increase in recrystallized grain sizes with increasing strain suggests that flow stress was lower in the more strained rocks.

INTRODUCTION

IN THIS paper, quartz *c*-axis fabrics in a pebbly metaquartzie (Elba Quartzite) are described and compared with strains determined from pebble shapes. Two suites of specimens were examined to determine the effects of strain intensity and shape of the strain ellipsoid on *c*-axis patterns. The results are similar to those of other studies of natural tectonites and also to those of experimental and computer simulation studies.

A large amount of experimental data has been published regarding the deformation of quartz and quartzite at high temperatures and confining pressures. Experimentally deformed quartzites are texturally similar to natural tectonites and have similar microfabric patterns (Tullis *et al.* 1973) but most of the experiments have been restricted to axial flattening deformations and thus are not directly comparable with more general, natural deformations. Tullis (1977), however, has published data from experiments in which approximately plane strain and 'simple shear' deformation occurred. These types of strain are probably more common in nature and are thus of greater significance for the interpretation of preferred orientations in natural tectonites.

Computer simulations of quartzite deformation were performed by Lister *et al.* (1978) for four models in which different combinations of active glide systems and their critical resolved shear stresses were considered. The model was that of Taylor–Bishop–Hill, in which multiple slip in original quartz grains is the only mechanism of deformation and grain reorientation. Different geometries of deformation were considered in the simulations and thus a wider range of deformation conditions was studied than is possible with present experimental techniques. At present, computer simulations have not accounted for the effects of recrystallization, although Lister & Price (1978) suggested that these effects are small and that the major reorienting mechanism in quartzite is slip.

Another possible method for determining the significance of crystallographic preferred orientations is to define the deformation history in natural tectonites as closely as possible and relate it to the measured microfabrics. In practice, it is rarely possible to define the deformation history even approximately, particularly in highly deformed tectonites, and thus the total strain and the structural history inferred from the small structures are commonly the only means available for estimating the strain history. Sylvester & Christie (1968) compared qualitatively determined flattening strains to quartz fabrics. Quantitative studies of the relation between strain and quartz fabrics were published by Marjoribanks (1976), Bouchez (1977), Tullis (1977) and Compton (1980). These studies established that the strength of preferred orientations increases with increasing strain and that different fabric patterns are produced by strains represented by different shapes of the strain ellipsoid.

STRUCTURAL SETTING

The Elba Quartzite is the basal unit of a clastic sequence that unconformably overlies Archaean basement in southern Idaho and northwestern Utah, U.S.A. The sequence in the northern Albion Mountains was sampled for this study; there it was metamorphosed to greenschist and amphibolite facies during the Mesozoic and Cenozoic and penetratively deformed during four events. Probably only two of these events produced appreciable strains in much of the Elba Quartzite: (a) ductile deformation of the metaclastic rocks above the

* Present address: U.S. Geological Survey, 345 Middlefield Road, Menlo Park, CA 94025, U.S.A.

stiff, underlying basement gneisses which involved at least a small amount of shear parallel to bedding and much flattening perpendicular to bedding and (b) warping above a dome in the gneisses. The latter deformation resulted in a marked variation of the strain intensity over the dome. Foliation is approximately parallel to bedding, and the dominant lineation in the foliation lies parallel to axes of common minor folds of nearly uniform N 40° W trend. A more detailed account of the structures and metamorphism is given elsewhere (Miller 1980).

DESCRIPTION OF ELBA QUARTZITE

The quartzite was metamorphosed to upper greenschist or lower amphibolite facies and was extensively recrystallized. Estimates of strain and measurements of the quartz microfabric were determined for specimens from a conglomerate unit in the Elba Quartzite. Photomicrographs of three specimens that underwent approximately plane strain are shown in Figs. 1, 2 and 3. The matrix of the conglomerate contains as major constituents, recrystallized quartz (75–90%), muscovite, and microcline porphyroclasts; minor amounts of biotite, epidote, garnet, and iron oxide minerals are also present. The pebbles are commonly pure quartz and are partly to fully recrystallized; some apparently were single crystals. They range from 0.5 to 5 cm in diameter for restored spherical shapes. Microcline porphyroclasts are broken and in part crystallized to muscovite in the specimens that experienced large strains. Elsewhere, muscovite occurs as tiny unbent flakes oriented parallel to foliation.

Subgrains are common, particularly in the large quartz grains and pebbles (Fig. 1). Grain boundaries range from straight to curved or slightly embayed and 120° triple junctions are common. Deformation lamellae are uncommon, and where present, in less than 1% of the grains, they are nearly parallel to basal planes.

Quartz grains in the pebbles are consistently larger than those in the more micaceous matrix surrounding the pebbles. In less strained specimens the distinction between pebble and matrix size is clear (Figs. 1 and 2), whereas in specimen 6 (the most highly strained specimen), the grain size is nearly homogeneous throughout the rock, and only a few pebbles have distinctly larger grain size than matrix grains (Fig. 3). Polycrystalline pebbles with the smallest grain size are those in samples that underwent the least strain, and the pebble grain size generally increases with higher strain intensity. A less well defined trend in the matrix grain size is similar to that in the pebbles, but quartz grain sizes in the matrix probably result from the spacing of micas and feldspars. Grain dimensions were measured in pure recrystallized quartz pebbles to study the relation between grain size and strain.

All matrix quartz grains are generally equant to slightly elongate parallel to foliation (subparallel to bedding), whereas pebble grains are approximately equant (Fig. 2). The scarcity of deformation lamellae and the generally equant quartz grain shapes suggest that the quartzite probably annealed at low stress or hydrostatic pressure.

STRAIN ANALYSIS

Strain was estimated in each oriented conglomerate specimen by combining average pebble ellipse shapes from each of three mutually perpendicular planes to obtain the strain ellipsoid. The calculation method was described by Oertel (1978) and Miller & Oertel (1979). It is assumed that: (1) the rock underwent no volume change, (2) no mechanical contrast existed between pebbles and matrix, (3) strain was homogeneous on the scale of the specimen and (4) the pebbles were initially spherical or ellipsoidal and randomly oriented. The first three assumptions are considered to result in little error. Uncertainties caused by the initially non-random orientation of ellipsoidal pebble shapes are probably the largest errors and are difficult to evaluate. Relative errors are probably greater in samples that were less deformed. Any initial preferred orientation of the pebbles probably resulted in the orientation of the minimum pebble dimensions approximately perpendicular to bedding. The strain measurements indicate that maximum shortening is approximately normal to bedding, and thus the samples may have been less flattened than the pebble shapes indicate. No attempt has been made to correct this error because the magnitude of the initial sedimentary shape anisotropy is impossible to determine.

Strains are listed in Table 1 and shown graphically in Fig. 4. The strains can be conveniently described in terms of a parameter proportional to the natural octahedral unit shear and here termed the "strain intensity" ($\mathscr{E}_s$) and Lode's parameter (ν), where

$$\mathscr{E}_s = 1/\sqrt{3}\,[(\mathscr{E}_1-\mathscr{E}_2)^2+(\mathscr{E}_2-\mathscr{E}_3)^2+(\mathscr{E}_3-\mathscr{E}_1)^2]^{1/2}, \quad (1)$$

Table 1. Measured strains and grain sizes in conglomerate from Elba Quartzite

Specimen number	Principal strains ϵ_1	ϵ_2	ϵ_3	Strain intensity	Lode's parameter	Grain size D (μm)	Twiss (1977)	Flow stress ($\sigma_1-\sigma_3$) (MPa) Mercier *et al.* (1977)	Christie *et al.* (1980)
19	0.77	−0.03	−0.42	0.79	−0.09	234	14.8	7.9	11.4
29	0.97	−0.03	−0.48	0.94	−0.08	381	10.6	5.6	5.5
9	1.28	−0.01	−0.55	1.15	−0.03	481	9.1	4.8	4.3
3	1.57	−0.16	−0.54	1.23	−0.31	439	9.6	5.1	4.7
2	1.09	0.29	−0.63	1.26	0.44	707	7.0	3.6	2.8
6	1.69	0.02	−0.63	1.41	0.02	374	10.7	5.7	5.7

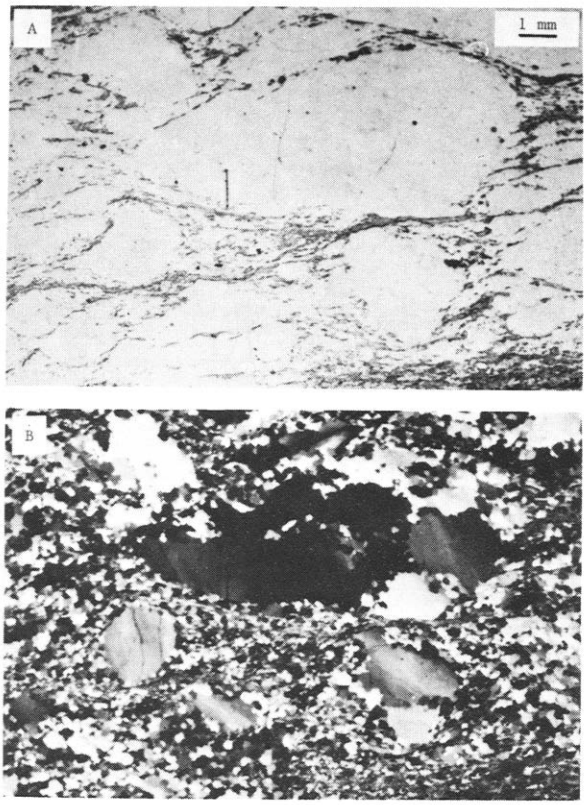

Fig. 1.

Fig. 1. Coarse-grained polycrystalline and single-crystal pebbles in micaceous, fine-grained matrix, specimen 19. Subgrains are distinctive in many of the pebbles. Trace of foliation in photo is horizontal and lineation is perpendicular to plane of photo. (a) plane polarized light; (b) crossed polarizers.

Fig. 2. Large recrystallized pebbles outlined by mica films, specimen 9. Matrix grains are larger than in specimen 19 (Fig. 1) and recrystallization in pebbles is more extensive. (a) plane polarized light; (b) crossed polarizers. Trace of foliation in photo is horizontal and lineation is in plane of photo. Pebble whose microfabric was examined is in lower right portion of photograph.

Fig. 3. Deformed feldspar porphyroclasts and highly recrystallized pebble and matrix quartz grains, specimen 6. Some feldspars are partially recrystallized to muscovite. Pebbles (outlined by mica films) contain quartz grains of size approximately equivalent to those in the matrix. (a) plane polarized light; (b) crossed polars. Photo is taken perpendicular to foliation and parallel to lineation. Vertical lines are imperfections in thin section.

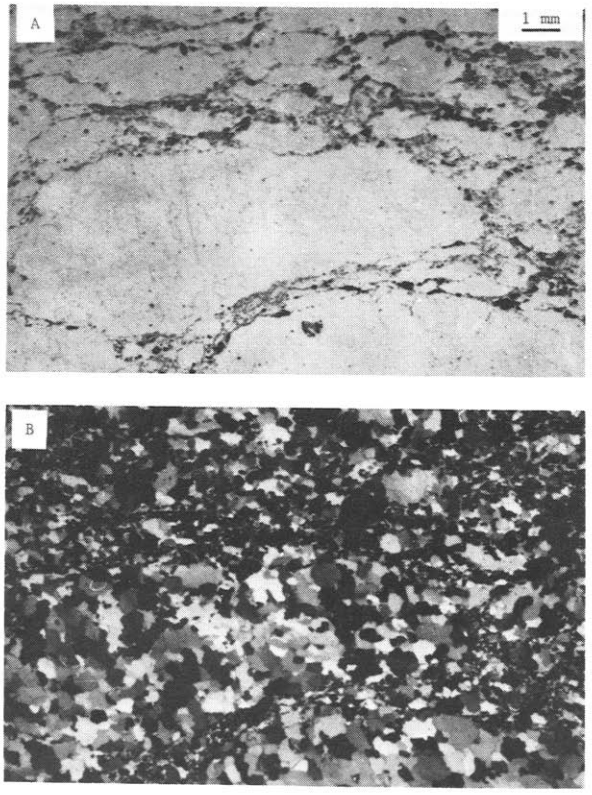

Fig. 2.

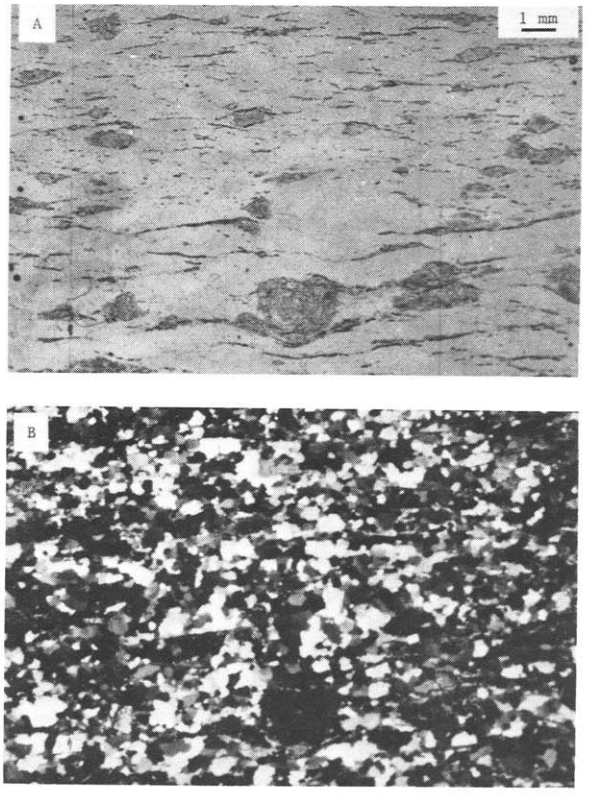

Fig. 3.

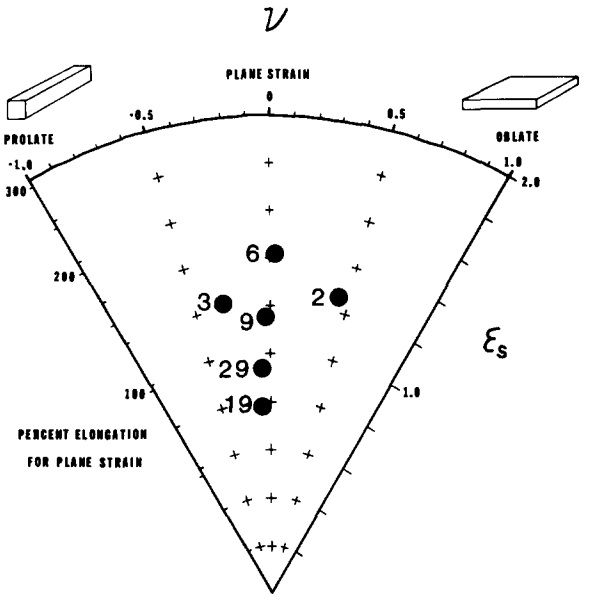

Fig. 4. Plot of strain intensity parameter ($\mathscr{E}_s$) vs Lode parameter (ν).

$$\nu = [(2\mathscr{E}_2 - \mathscr{E}_3)/(\mathscr{E}_1 - \mathscr{E}_3)] - 1 \quad (2)$$

The $\mathscr{E}_i$ are logarithmic (natural) strains defined by

$$\mathscr{E} = \ln(1 + \epsilon_i) \quad (3)$$

where the principal strains (ϵ_i) are defined such that ϵ_1 is the direction of maximum extension. Nadai (1963, p. 73) derived the expression for the strain intensity parameter; it is proportional to distortion of the strain ellipsoid and is useful for comparing strain intensities for different shapes of the strain ellipsoid. Lode's parameter (Lode 1926, p. 932) describes the shape of the strain ellipsoid.

MICROFABRIC MEASUREMENT AND REPRESENTATION

The orientations of quartz *c*-axes were measured in each sample by standard universal stage techniques (Turner & Weiss 1963). Because strain the specimens appears to be relatively homogeneous on the scale of the specimen (10–30 cm) but less so on the scale of individual pebbles (1–4 cm), *c*-axes were measured in two thin sections prepared from each of two mutually perpendicular surfaces cut perpendicular to foliation. Thus a more representative sample of *c*-axes was measured than would generally be possible from only two thin sections. Grains within the matrix were measured separately from those in individual pebbles since *c*-axes in the pebbles may have had preferred orientations prior to their deposition. Matrix quartz grains are used for comparative purposes between samples because any initial preferred orientations in pebbles are expected to limit their usefulness. Matrix grains were measured along traverses perpendicular to foliation; those grains adjacent to pebbles were not measured.

The preferred orientations of quartz *c*-axes are depicted in lower hemisphere, equal-area projections and contoured by a modification of the method described by Kamb (1959). His method entails choosing a counting area such that the expected number of points (E) within the area is three times the standard deviation of the number of points that will actually fall in the area for a randomly distributed population ($E = 3\sigma$). This method results in contours that lack much of the detail of those generated by the standard Schmidt method (Turner & Weiss 1963). In order to retain some of this detail, the counting area in this study was chosen such that $E = 2\sigma$. The data were rotated and contoured by a computer program that was developed by Miller (in part modifed from a program by G. Dollinger). The program determines the counting area from the size of the sample to be contoured and then counts the number of points within this area as the counter moves over a grid on a spherical projection. The number of points thus counted is printed on an equal-area plot and they are contoured in multiples of the standard deviation (multiples of the expected number $E = 2\sigma$ for a uniform distribution) on a similar plot. Rotations are also performed by the computer.

Two suites of conglomerate specimens were studied. The first consists of four specimens (Nos 6, 9, 19 and 29) that were subjected to approximately plane strain of different intensities ($\mathscr{E}_s$ ranges from 0.79 to 1.41). The second suite consists of three specimens (Nos 2, 3 and 9) of approximately equivalent strain intensity ($\mathscr{E}_s \cong 1.2$) with different shapes of the strain ellipsoid (ν ranges from -0.31 to $+0.44$; the former is a prolate and the latter an oblate ellipsoid). The strains measured in the specimens are shown in Fig. 4.

Contoured plots of 400 quartz *c*-axes were prepared for each specimen. Smaller samples of 200 grains were plotted separately for each specimen in order to obtain an indication of the reproducibility of the patterns shown on the contoured plots. These tests of reproducibility are discussed below. Contoured plots of grains from polycrystalline pebbles were also prepared for comparison with the matrix grain plots.

PREFERRED ORIENTATIONS IN THE MATRIX

Effect of the strain intensity

Fabric diagrams in Fig. 5 represent the suite of samples that were subjected to plane strains of different intensities. The patterns are poorly defined two-girdle patterns, symmetrical to ϵ_1, with maxima generally at the intersections of the girdles and perpendicular to ϵ_2, and with pole-free areas near the ϵ_1 axis. One girdle for specimen 6 is more strongly developed than other, perhaps as a result of rotational strain as simulated by Lister (1977). Other diagrams are suggestive of similar asymmetry, but they are more complex in detail and do not lend themselves to such a simple interpretation. The opening half-angle (half the dihedral angle between the planes represented by the girdles, measured such that it includes ϵ_3) is acute. Lister

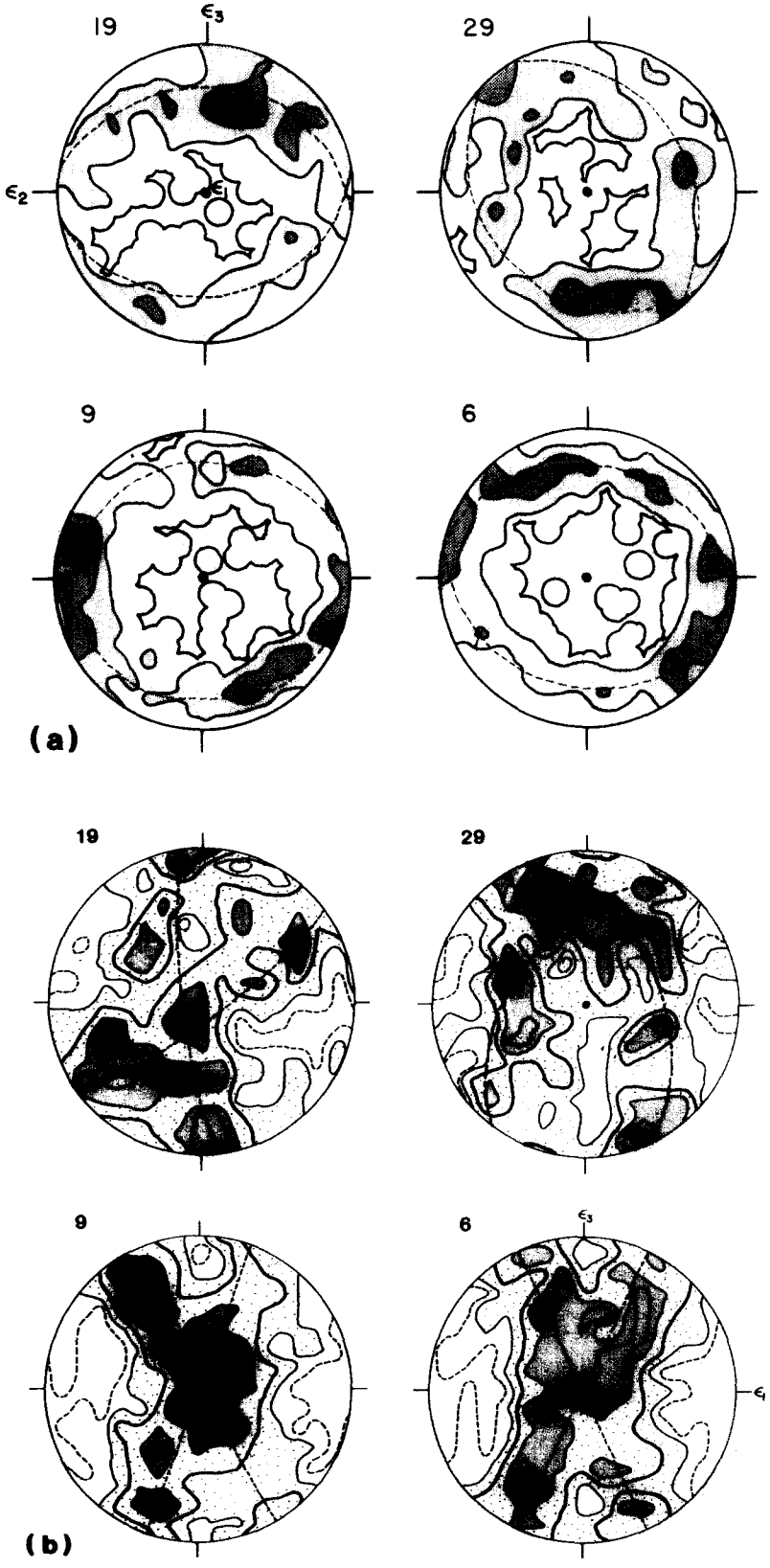

Fig. 5. Microfabric data from the matrix grains of conglomerate specimens of the Elba Quartzite that underwent approximately plane strain. Each diagram is a lower-hemisphere, equal area plot of 400 quartz *c*-axes. Contours are in multiples of the expected number of points for a uniform distribution; the counting area is 0.01 of the total area. (a) maximum principal strain vertical. Scalloped line outlines the pole-free area (contoured by the Mellis method), other lines represent multiples of the expected number. (b) intermediate principal strain vertical. Dashed line outlines the pole-free area, heavy line represents the expected number (2σ), and other lines are multiples of 1σ ($\frac{1}{2}$ the expected number).

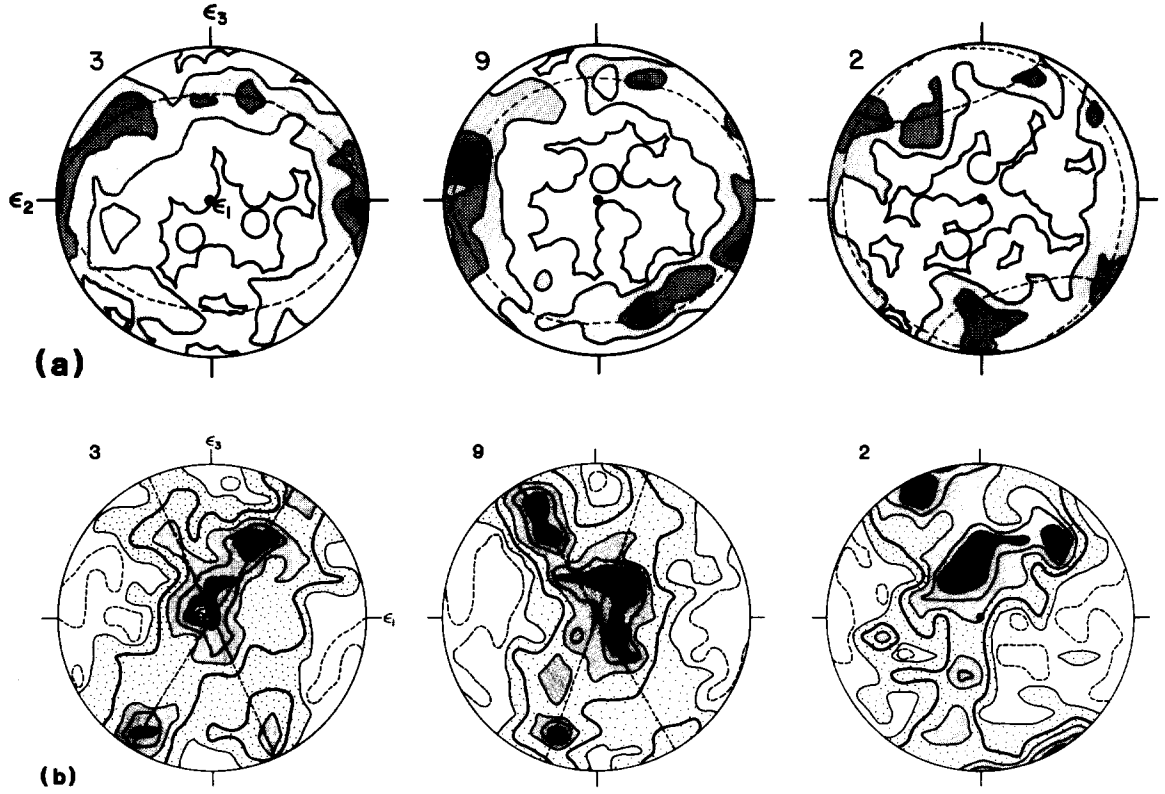

Fig. 6. Microfabric data from the matrix grains of conglomerate specimens of the Elba Quartzite that have measured strain intensity parameters approximately equal to 1.2 and differing values of Lode's parameter. Diagrams contoured as described in Fig. 5. Plots are oriented as shown for specimen 3.

(1977) and Tullis (1977) suggested that crossed-girdle patterns can be classified as two types: type I girdles consist of small-circle girdles about the ϵ_3 axis with connecting concentrations through the ϵ_2 axis; type II girdles consist of two great-circle girdles that intersect in a maximum at the ϵ_2 axis. The preferred orientation patterns in this suite of samples (Fig. 5) are similar to type II crossed-girdle patterns.

Orthorhombic symmetry is approximately displayed by the patterns in Fig. 5 but the symmetry is not well developed in the less strained specimens. Fabric patterns for specimens 9 and 6 are approximately symmetrical to the planes of principal strain, whereas the symmetry planes contain ϵ_2 in the other patterns but are misoriented with respect to the other principal strains. The half-angle between girdles, measured across ϵ_3, is approximately constant in the samples at 25 to 30°, but the girdles are defined more clearly with increasing strain intensity. Small misorientations between the symmetry planes and principal strains for specimens 6 and 9 are probably insignificant, but larger misorientations exist for specimens 29 and 19.

Effect of the shape of the strain ellipsoid

Specimens 3, 9 and 2 in Fig. 6 have similar strain intensities ($\mathscr{E}_s \cong 1.2$), and the measured strain ellipsoid shapes range from mildly extended to moderately flattened. Extreme shapes (axially shortened and extended) are not represented among the rocks in this area. Specimen 9 represents plane strain, and the *c*-axis pattern is a type II crossed-girdle pattern. Specimen 3, which was moderately extended, displays a fabric pattern similar to the type II crossed-girdle pattern in specimen 9 but one girdle is developed better than the other. Specimen 2 is moderately flattened, and its fabric pattern differs; *c*-axes are distributed in the plane containing ϵ_2 and ϵ_3 and several concentrations are present within about 60° of the ϵ_3 axis. The several maxima at moderate angles to the ϵ_3 axis might be taken as suggestive of a small-circle distribution, and the pattern therefore resembles a type I crossed-girdle pattern. The preferred orientations of quartz *c*-axes in specimens 2, 3 and 9 are approximately of the same strength, on the basis of estimates of the area enclosed by contours of equal *c*-axis density.

PREFERRED ORIENTATIONS IN THE PEBBLES

The microfabric patterns of quartz *c*-axes in the matrix and pebbles of specimens 9 and 29 are compared in Fig. 7. In each specimen 200 grains on a large pllycrystalline pebble were measured. The *c*-axis patterns for the pebbles consist of a strong maximum with subordinate maxima and partial girdles. The pebble fabric patterns show much stronger preferred orientations than the matrix patterns,

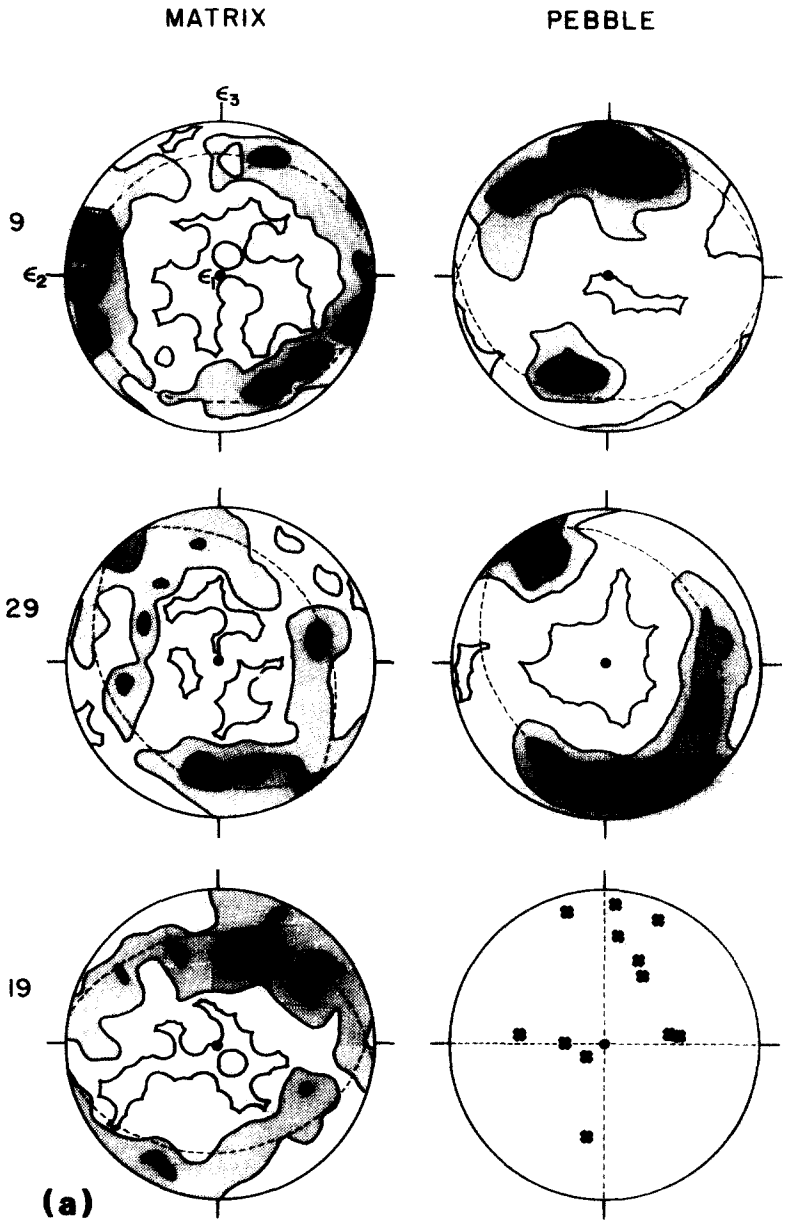

Fig. 7(a). Caption opposite.

but the incomplete girdles shown by fabrics in the pebbles coincide with those for the matrix. Unpublished fabric data measured by E. Idiz from pebbles in specimen 3 indicate similar relations.

The *c*-axis orientations of 12 nearly spherical single-crystal pebbles in specimen 19 were measured. The crystals are nearly undeformed, as indicated by few subgrains and small misorientations among the subgrains, compared to pebbles with elliptical sections. The *c*-axes of the undeformed pebbles are approximately oriented in two planes containing the principal strain axis and intersecting at the ϵ_1 axis (Fig. 7). Thus the orientation of the principal planes of strain seem related to the *c*-axes of relatively undeformed and unrecrystallized single-crystal pebbles in this moderately strained specimen.

REPRODUCIBILITY OF THE PREFERRED ORIENTATIONS

The sample size is important in measuring microfabrics because a sample must be large enough to smooth out the effects of local heterogeneous domains. In the specimens studied, two problems contribute to the difficulty of determining how large a sample is necessary. (1) Pebbles that were less deformed than, and therefore stiffer than, the matrix probably interfered with each other and caused heterogeneous strain in the matrix adjacent to and between pebbles. The matrix fabric patterns, therefore, may vary according to the different regions sampled near pebbles and their relation to pebble boundaries. (2) Large detrital grains or pebbles are recrystallized in some

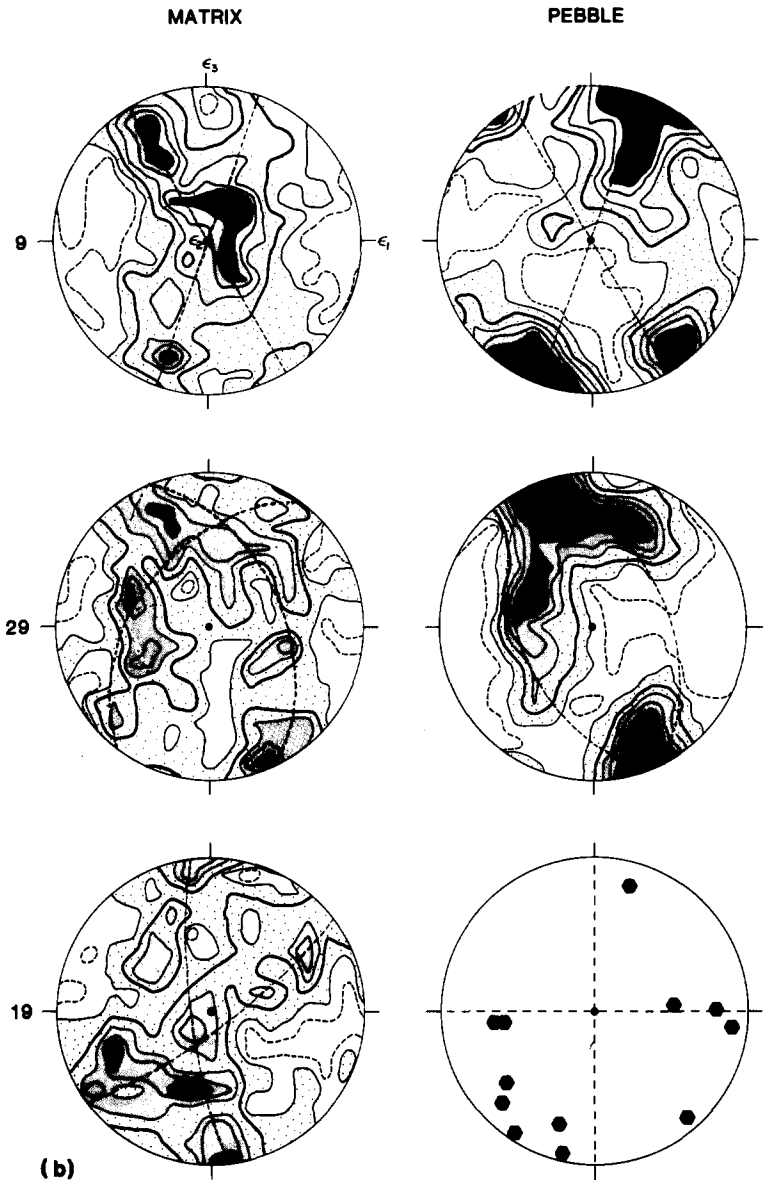

Fig. 7(b).

Fig. 7. Comparison of microfabrics in matrix and pebbles. Plots of quartz *c*-axes in matrix of samples 9 and 29 are contoured as described for Fig. 5a; 200 quartz *c*-axes are represented in each plot of pebble *c*-axes and the counting area for these plots is 0.02. Maximum concentrations for the pebble plots are 10σ for specimen 9 and 12σ for specimen 29. The orientations of 12 undeformed or slightly deformed single-crystal pebbles in sample 19 are indicated. Plots are oriented as shown for specimen 9.

specimens and are difficult to recognize; traverses across these regions yield several similar orientations. In order to test the adequacy of the sample size chosen for this study (400 grains), fabrics from the matrix grains in all specimens were compared for two samples of 200 before they were combined to form the diagrams in Figs. 5 and 6. In general, preferred orientations in specimens subjected to strains with $\epsilon_s > 1.0$ show good reproducibility (Fig. 8, specimen 9, is a representative example), and therefore the combined data (400 *c*-axes) for these specimens are considered to be representative. The precise localities and strengths of maxima in these diagrams, as well as in the diagrams representing grains measured in mutually perpendicular thin sections, are not reproduced. This effect is probably caused by local concentrations of *c*-axes in large, recrystallized grains.

Reproducibility of the preferred orientation patterns for 200 *c*-axes is poorer in less strained specimens, so a second set of 400 *c*-axes was measured in specimen 19, which is the least strained. Comparison of the fabric patterns based on 400 *c*-axes (Fig. 8) indicates that the girdle orientations are moderately well defined and the strongest concentrations of *c*-axes are reproduced. The fabric pattern is less clearly defined in the second data set, which was measured in thin sections that contain approximately three times the number of pebbles contained in those for the first set. For this reason, the first set was used in Figs. 5 and 6. The preferred orientation pattern of the

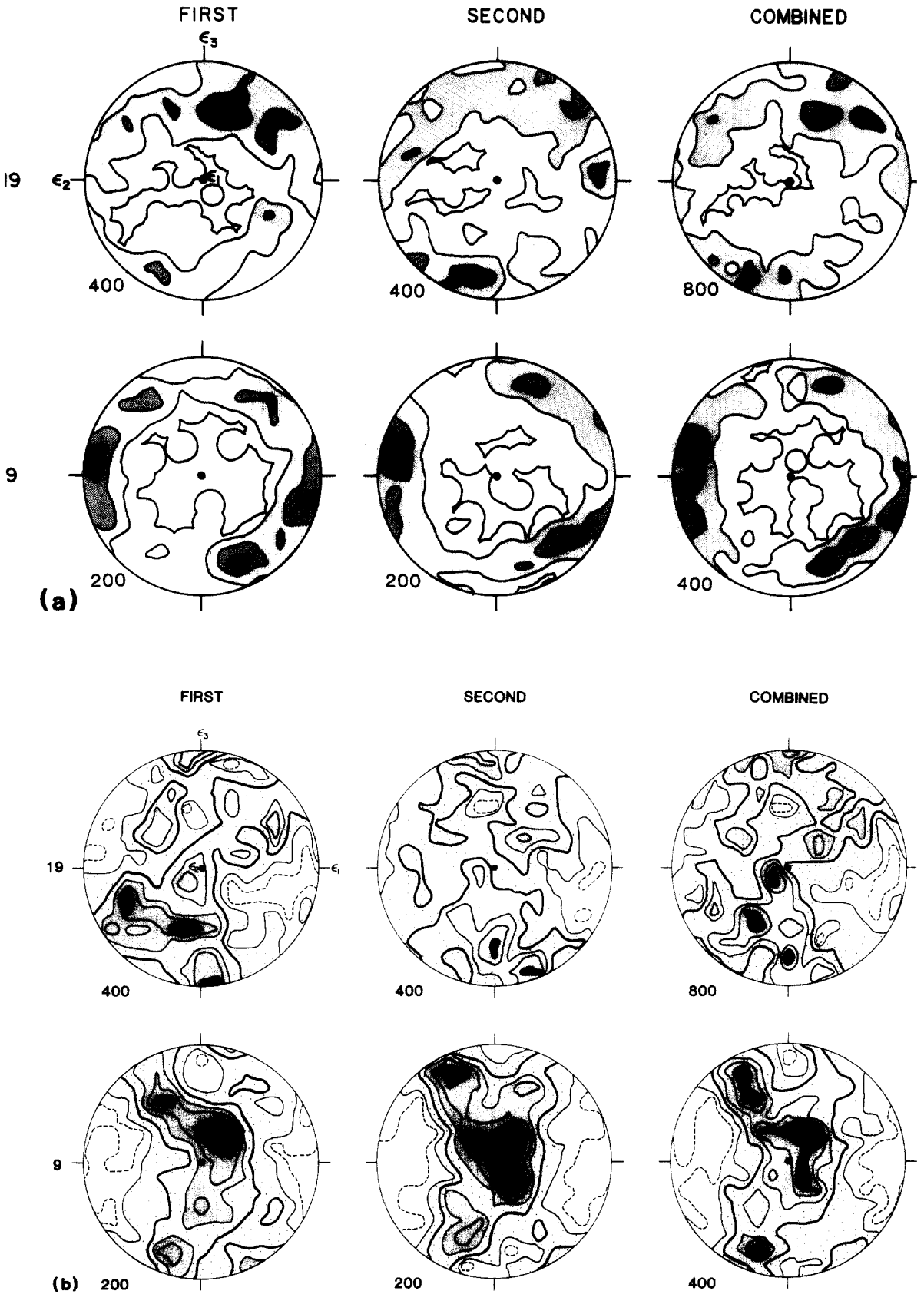

Fig. 8. Test of reproducibility of data for specimens 19 and 9. The number of *c*-axes measured are indicated below each diagram. First and second data sets for specimen 19 are contoured as described in Fig. 5(a), and the combined data are contoured using a counting area of 0.005; contours are in multiples of the expected number for a uniform distribution. First and second data sets for specimen 9 are contoured using a counting area of 0.02. The combined data are contoured as in Fig. 5(a). Orientations of plots are as in Fig. 5.

combined (800) c-axes is similar to that of the first data set and we thus consider that 400 c-axes is adequate for determining the shapes and orientations of girdles and the locations of major concentrations of c-axes in specimens with relatively low strains ($\mathscr{E}_s < 1.0$).

GRAIN SIZE

Grain dimensions were measured in fully recrystallized, pure quartz pebbles by counting the number of grain boundaries intersecting a line of known length for three orthogonal orientations of the line. The geometric mean of the grain intercepts was then adjusted to account for grain volumes:

$$D = 3/2\,\bar{N}_L \quad (4)$$

where $\bar{N}_L$ is the mean grain intercept and D the adjusted grain size. Sizes of grains in 4 to 6 pebbles were calculated for each specimen; the mean of these measurements is given in Table 1. Grain size is smallest in the least strained specimen (19) and generally increases with increasing strain. A notable exception to this trend is the most highly strained rock (6), which has a relatively small grain size. The pebbles in this sample are difficult to identify in thin section (Fig. 3) and commonly contain scattered micas and iron oxide crystals as impurities. Impurities in the pebbles in this specimen may have limited grain growth and hence the final size of the quartz grains. This phenomenon is commonly observed in micaceous quartzites and it is well known that crystalline impurities limit grain growth in metals.

INTERPRETATION

Relation between preferred orientation and strain

This study has shown that the strength of quartz c-axis preferred orientation increases with increasing plane strain. Previous studies have documented similar trends for flattening strains (Sylvester & Christie 1968, Compton 1980) and moderate extension (Bouchez 1977). Lister *et al.* (1978) found the same result for computer models of plane strain resulting from dislocation glide. Since the recrystallized quartzites in this study show the same trend, any effects of recrystallization that would tend to diffuse the preferred orientations appear to be small compared to the processes that strengthen them, as was suggested by Lister & Price (1978).

The relation between preferred orientation patterns and the shapes of the strain ellipsoids in this study is ambiguous. Moderately extended quartzites with type I crossed girdle patterns are documented by Marjoribanks (1976) and Tullis (1977), but axial extension produced small circles with opening angles of about 75° about the direction of maximum extension in computer models of dislocation glide (Lister *et al.* 1978). Marjoribanks (1976) and Tullis (1977) document type I crossed girdles in unrecrystallized tectonites subjected to plane strains. Similar results were obtained by Tullis (1977) in original grains that were experimentally deformed and by Lister *et al.* (1978) and Lister & Price (1978) in computer simulations involving dislocation glide. Moderate flattening strains were shown by Marjoribanks to have resulted in type I crossed-girdle patterns, and similar results were obtained from computer simulations of polycrystal deformation by dislocation glide (Lister & Price 1978). Experiments resulting in axial shortening (Tullis *et al.* 1973) and computer simulations for similar strains (Lister *et al.* 1978) produced small-circle distributions about the shortening axis. Although preferred orientation patterns differ somewhat for strains representing various shapes of the strain ellipsoid, these differences as documented by Marjoribanks (1976) and Bouchez (1977) are not systematic nor are they always in accord with results from experimental and computer simulation studies. We consider that since the observed differences are small, they may reflect factors other than total strain, such as the strain history. In computer simulations (Lister & Price 1978), late strains rapidly modify fabrics formed during earlier strains, and the resulting fabrics may thus predominantly reflect the geometry of the late strain rather than the total strain.

Misorientations between symmetry planes in fabric diagrams and the planes of principal strain are demonstrated in this study. Similar results were obtained by Marjoribanks (1976, fig. 11, specimens 9a, 26 and 17). The probable cause of this misorientation is that the fabrics chiefly reflect the last stage of strain in a non-coaxial strain history, whereas strains determined from the pebble shapes represent the entire deformation. Further support for a locally non-coaxial strain history is evident in the asymmetrical development of girdles in patterns for specimens 6 and 3. The remainder of the specimens also exhibit asymmetrical girdles, but the asymmetry is less clearly defined. The sense of shear indicated by the girdle asymmetry is incompatible with strains inferred from minor structures that developed during the two phases of penetrative deformation thought to have affected the Elba Quartzite. We therefore conclude that the asymmetry represents strain during a portion of a complex, non-coaxial strain history; perhaps the strain was rotational for this part. Asymmetry in the less strained specimens may in part reflect inhomogeneities in the sampled quartz grains in small regions of the rock.

The orientations of essentially undeformed single-crystal pebbles in specimen 19 are of interest in the light of the observation by Tullis *et al.* (1973) that c-axes in relatively undeformed grains are oriented parallel and perpendicular to the direction of maximum compressive stress in axial shortening experiments (i.e. the orientations giving zero resolved shear stress for basal slip). The data for specimen 19 therefore suggest that the principal stresses were approximately parallel to the principal strains (i.e. strain was non-rotational). Unrecrystallized and undeformed pebbles are less common in the more highly deformed specimens, perhaps because the rocks experienced more rotation of the principal stresses during deformation or because of more extensive recrystallization.

Grain size

On the basis of experimental studies of deformed quartzite, Mercier *et al.* (1977) showed that recrystallized grain size was related inversely to flow stress during steady state flow. Twiss (1977) derived a theoretical relation between grain size and flow stress. More recent experimental data from quartzites deformed to steady state in hydrous assemblies with high partial pressures of H_2O (Christie *et al.* 1980) differ from these estimates in the experimental range. An updated analysis of these data (Christie, Ord & Koch 1980, personal communication) yield the relationship $\sigma = 40.9 \times d^{-1.11}$ (or $D = 28.2 \times \sigma^{-0.9}$). These data may be used to estimate flow stressers for the Elba Quartzite if the deformation of the quartzite resulted in complete recrystallization and achieved steady state flow. The absence of detrital grains in Elba Quartzite, other than large single crystal pebbles, indicates that recrystallization was complete in the polycrystalline pebbles and matrix.

Textures in the Elba Quartzite are qualitatively similar to those of quartz rocks experimentally deformed at high temperatures and also to those of deformed samples experimentally annealed after deformation. It should be emphasized that flow stresses inferred from grain sizes will reflect a true flow stress only in special circumstances: namely, if the grain size equilibrated with stress $(\sigma_1 - \sigma_3)$ under 'hot-working' conditions (syntectonic recrystallization) and the rock was then cooled under the same stress below a temperature at which grain boundaries are no longer mobile. Hydrostatic annealing or a temporary change of stress will tend to cause a change of grain size. In particular, hydrostatic annealing after deformation, especially over long periods of time ($\sim$Ma), will cause significant grain growth, so that flow stresses inferred from grain size will be significantly underestimated.

Flow stresses determined from the grain sizes using the equations of Mercier *et al.* (1977) and Twiss (1977) for the stress–grain size relationships are given in Table 1. The stresses derived from the Twiss relation range from 7 to 15 MPa and those from the Mercier *et al.* data are between 3 and 8 MPa. The relationship of Christie *et al.* (1980) quoted above gives flow stresses in the same range (between 2.8 and 9.5 MPa). It is noteworthy that the flow stresses decrease, in general, with increasing strain intensity in the samples. However, the stresses inferred for different samples vary only by a factor of 2 and it is not clear that the inverse relationship between the inferred stresses and strains is significant.

We have no independent criteria for establishing the temperature or duration of the deformation events in the area. The rocks are of greenschist and amphibolite facies and the greater degree of crystallization of white mica from microcline in the more highly strained specimens suggests that these specimens were hotter. For steady state flow in any rock, the flow stress at a given strain rate decreases, or the strain rate at a given stress increases, with increasing temperature. Thus the association of lower flow stress and higher strains (due to faster strain rates) in hotter rocks is quite consistent with experimental observations.

However, we note that the pebble shapes record the accumulated strain during all (or most) of the strain history, whereas the grain sizes were established during the last recrystallization event. The latter event was metamorphism associated with deformation of the rocks into a dome, probably associated with diapiric emplacement of an underlying granitic stock. The strains recorded in the quartzites range symmetrically with respect to the dome (Miller 1980) and it therefore appears likely that most of the strain was produced during this latest doming event, along with the recrystallization. Thus the inverse relationship between flow stress and strains may be significant, reflecting faster strain rates and lower flow stress in the hotter rocks than the cool ones during the doming events.

The maximum temperatures in the hottest rocks sampled were probably >500°C, which suggests that temperatures high enough for significant annealing and grain growth (at least in the hottest rocks) may have prevailed for long periods. For this reason the stresses inferred from grain sizes are probably minimum estimates of the flow stresses in the rocks during the coming event.

DISCUSSION

The absence of parallelism between the microfabric symmetry planes and the principal planes of strain has important implications for the interpretation of these data. A number of factors affect the preferred orientations that develop as a result of general strain. Among these are the relative importance of different slip systems, the presence and importance of diffusive deformation mechanisms, nucleation and growth of grains during recrystallization, the strain history, the abundance of other mineral phases, and the original orientation of the grains. For a simple strain history in which the stress applied is constant and the strain is non-rotational, it is expected that only an original non-uniform *c*-axis distribution would result in a misorientation between the microfabric symmetry planes and the principal planes of strain. At large strains this effect would decrease. Because the highly strained quartzites studied here show such a misorientation we conclude that a complex strain history caused this effect. This conclusion is supported by asymmetrical girdles in some fabric diagrams, as well as by the evidence from small-scale structures for two periods of strong deformation of markedly different 'style' over parts of the area.

Despite the complex strain histories of some of the specimens, the direct relationship between strength of preferred orientation and strain intensity suggests that the strength of preferred orientations in nearly monomineralic rocks may be a useful qualitative indicator of strain intensity. In order for such a correlation to be valid, the microfabrics should be measured in relatively pure quartz rocks to avoid the effects of variable amounts of impurities. The area sampled must be small enough that a generally similar strain geometry and strain history can be demonstrated for all of the samples.

Acknowledgements—Support at UCLA was provided by Earth Sciences Section, National Science Foundation Grant EAR 76-14758 to J. M. Christie and C. A. Nelson. Miller acknowledges the support of the U.S. Geological Survey, under whose tenure part of this study was completed. Review of this paper at various stages by J. Tullis, G. Oertel, S. Kirby and R. Loney is gratefully acknowledged. R. Alkaly and J. DeGrosse prepared the thin sections.

REFERENCES

Bouchez, J.-L. 1977. Plastic deformation of quartzites at low temperature in an area of natural strain gradient. *Tectonophysics* **39,** 25–50.

Christie, J. M., Ord. A. & Koch, P. S. 1980. Relationship between recrystallized grain size and flow stress in experimentally deformed quartzite. *Trans. Am. geophys. Un.* **61,** 377.

Compton, R. R. 1980. Fabrics and strains in quartzites of a metamorphic core complex, Raft River Mountains, Utah. In: *Cordilleran Metamorphic Core Complexes* (edited by Crittenden, M. D., Jr., Coney, P. J. & Davis, G. H.). *Mem. Geol. Soc. Am.*, **153,** 385–398.

Kamb, W. B. 1959. Ice petrofabric observations from Blue Glacier, Washington, in relation to theory and experiment. *J. geophys. Res.* **64,** 1891–1909.

Lister, G. S. 1977. Discussion: Crossed girdle *c*-axis fabrics in quartzites plastically deformed by plane strain and progressive simple shear. *Tectonophysics* **39,** 51–54.

Lister, G. S., & Price, G. P. 1978. Fabric development in a quartz-feldspar mylonite. *Tectonophysics* **49,** 37–78.

Lister, G. S., Paterson, M. S. & Hobbs, B. E. 1978. The simulation of fabric development in plastic deformation and its application to quartzite: the model. *Tectonophysics* **45,** 107–158.

Lode, W. 1926. Versuche uber den Einfluss der mittleren Haupispannung auf das Fliessen der Metalle Eisen, Kupfer und Nickel. *Zeitschrift fuer Physik* **36,** 913–939.

Marjoribanks, R. W. 1976. The relation between microfabric and strain in a progressively deformed quartzite sequence from central Australia. *Tectonophysics* **32,** 269–293.

Mercier, J. C., Anderson, D. A. & Carter, N. L. 1977. Stress in the lithosphere; inferences from steady state flow of rocks. *Pure appl. Geophys.* **115,** 199–226.

Miller, D. M. 1980. Structural geology of the northern Albion Mountains, south-central Idaho. In: *Cordilleran Metamorphic Core Complexes* (edited by Crittenden, M. D., Jr., Coney, P. J. & Davis, G. H.) *Mem. Geol. Soc. Am.* **153,** 399–424.

Miller, D. M. & Oertel, G. 1979. Strain determination from the measurement of pebble shapes: a modification. *Tectonophysics* **55,** T11–T13.

Nadai, A. 1963. *Theory of Flow and Fracture of Solids.* Vol. 2. McGraw-Hill, New York.

Oertel, G. 1978. Strain determination from the measurement of pebble shapes. *Tectonophysics* **50,** T1–T7.

Sylvester, A. G. & Christie, J. M. 1968. The origin of crossed-girdle orientations of optic axes in deformed quartzites. *J. Geol.* **76,** 571–580.

Tullis, J. 1977. Preferred orientation of quartz produced by slip during plane strain. *Tectonophysics* **39,** 87–102.

Tullis, J., Christie, J. M. & Griggs, D. T. 1973. Microstructures and preferred orientations of experimentally deformed quartzites. *Bull. geol. Soc. Am.* **84,** 297–314.

Turner, F. J. & Weiss, L. E. 1963. *Structural Analysis of Metamorphic Tectonites.* McGraw-Hill, New York.

Twiss, R. J. 1977. Theory and applicability of a recrystallized grain size paleopiezometer. *Pure appl. Geophys.* **115,** 227–244.